Discovery of a Superhard Iron Tetraboride Superconductor

Huiyang Gou,[1,2] Natalia Dubrovinskaia,[2,*] Elena Bykova,[1,2] Alexander A. Tsirlin,[3,4] Deepa Kasinathan,[3] Walter Schnelle,[3] Asta Richter,[5] Marco Merlini,[6] Michael Hanfland,[7] Artem M. Abakumov,[8] Dmitry Batuk,[8] Gustaaf Van Tendeloo,[8] Yoichi Nakajima,[1] Aleksey N. Kolmogorov,[9] and Leonid Dubrovinsky[1]

[1]*Bayerisches Geoinstitut, Universität Bayreuth, D-95440 Bayreuth, Germany*
[2]*Laboratory of Crystallography, Material Physics and Technology at Extreme Conditions, University of Bayreuth, D-95440 Bayreuth, Germany*
[3]*Max Planck Institute for Chemical Physics of Solids, Nöthnitzer Straße 40, D-01187 Dresden, Germany*
[4]*National Institute of Chemical Physics and Biophysics, Akadeemia tee 23, 12618 Tallinn, Estonia*
[5]*Technische Hochschule Wildau, Bahnhofstraße 1, D-15745 Wildau, Germany*
[6]*Dipartimento di Scienze della Terra, Università degli Studi di Milano, Via Botticelli 23, 20133 Milano, Italy*
[7]*ESRF, Boîte Postale 220, 38043 Grenoble, France*
[8]*EMAT, University of Antwerp, Groenenborgerlaan 171, B-2020 Antwerp, Belgium*
[9]*Department of Physics, Applied Physics and Astronomy, Binghamton University, State University of New York, Vestal, New York 13850, USA*

(Received 22 February 2013; published 7 October 2013)

Single crystals of novel orthorhombic (space group *Pnnm*) iron tetraboride FeB_4 were synthesized at pressures above 8 GPa and high temperatures. Magnetic susceptibility and heat capacity measurements demonstrate bulk superconductivity below 2.9 K. The putative isotope effect on the superconducting critical temperature and the analysis of specific heat data indicate that the superconductivity in FeB_4 is likely phonon mediated, which is rare for Fe-based superconductors. The discovered iron tetraboride is highly incompressible and has the nanoindentation hardness of 62(5) GPa; thus, it opens a new class of highly desirable materials combining advanced mechanical properties and superconductivity.

DOI: 10.1103/PhysRevLett.111.157002 PACS numbers: 74.70.Ad, 61.05.cp, 62.20.-x, 62.50.-p

Modern computational materials design is gaining broad recognition as an effective means of reducing the number of experiments that can ultimately lead to materials discovery [1–3]: successful examples now include thermoelectrics, catalysts, electrode materials for Li-ion batteries, to name a few. Superconductors remain among the most challenging materials to develop [2,4–6]. So far theory has only successfully guided experiment to a discovery in a few cases related to thoroughly studied elemental materials, namely, silicon [7] and lithium [8] under pressure. The progress can be attributed to the improvement of density functional theory-based methods [9,10], advances in compound prediction strategies [1,3], and the steady growth of computational resources. Nevertheless, the prediction of novel superconductors remains challenging [4]. First, only conventional (phonon-mediated) superconductors are understood well enough [4] to be described by theories with predictive power [5,11]. Calculation of the superconducting critical temperature, T_c, is possible but exceedingly demanding as a viable option in high-throughput screening for candidate materials. Second, the inverse correlation between the stability of a compound and its phonon-mediated superconducting T_c has been pointed out in a number of studies: a considerable density of states (DOS) at the Fermi level, beneficial for high T_c, is often an indication of structural instability [6]. One of the remarkable exceptions is the stoichiometric MgB_2 material [12] with naturally hole-doped σ bands and a T_c of 39 K.

The problem of thermodynamic instability can be mitigated under high pressure. When quenched to normal conditions, materials with a large DOS at the Fermi level may remain metastable and show superconductivity facilitated by this large DOS. Kolmogorov *et al.* [9] systematically examined the Fe-B system and showed that a previously unknown compound, FeB_4, may exist under normal conditions in a previously unobserved orthorhombic crystal structure. The material was predicted to have naturally electron-doped bands and a large electron-phonon coupling [9], which indicate that FeB_4 might be a "conventional" Fe-based superconductor (rare cases are known, see [13–15]), as opposed to the recently discovered family of "unconventional" Fe-based superconductors [2,16]. Bialon *et al.* [17] suggested that the predicted FeB_4 phase could be synthesized under pressure. The wide and growing interest in Fe-based superconductors [2], simple chemical composition, and expected mild pressure-temperature conditions for synthesis [17] make iron tetraboride a good case for testing the computational predictive power and, thus, the degree of our theoretical comprehension of such a complex physical phenomenon as superconductivity. Here, we report synthesis of an iron boride with a so-far unknown composition, the verification of theoretical predictions regarding the structure and superconductivity of this material, and the finding of its unexpectedly low compressibility and very high hardness.

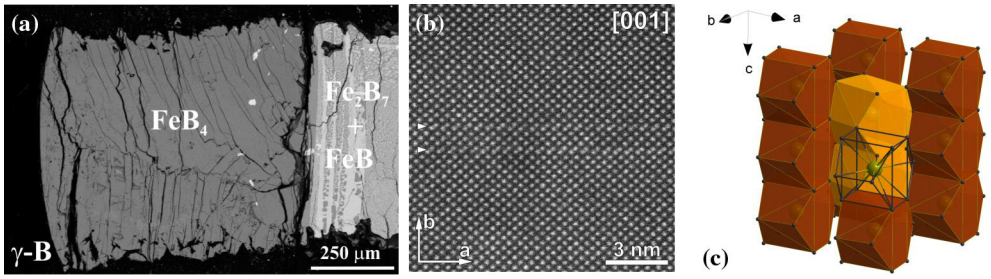

FIG. 1 (color online). (a) The backscattered electron SEM image of the polished surface of a high-pressure sample. The central part of the image (dark gray field) represents FeB_4 produced by the reaction of Fe with B after melting. The adjacent area on the right appears brighter as it is composed of the phases with lower boron content, namely, Fe_2B_7 and FeB. The surrounding black field is nonreacted boron which, however, underwent a pressure-induced phase transformation from β-B to γ-B. Boron intrusions also fill the cracks in the FeB_4 phase. (b) The high resolution [001] HAADF-STEM image of FeB_4 (bright dots correspond to the Fe columns). Occasional planar defects (marked with arrowheads) are confined to the (010) plane and are visible as lines running parallel to the a axis and consisting of pairs of the Fe columns with a shorter projected intercolumn distance in comparison with the FeB_4 matrix [25]. (c) Crystal structure of FeB_4 presented as a packing of columns of FeB_{12} polyhedra along the c direction; the columns are connected by common edges of the adjacent polyhedra, whose centers (Fe atoms) are displaced with respect to each other by $1/2$ along the body diagonal of the unit cell.

The experimental Fe-B phase diagram [18] at ambient pressure shows only two compounds, tetragonal Fe_2B and orthorhombic FeB (Ref. [19]), although hexagonal FeB_2 (Ref. [20]) and rhombohedral $FeB_{\sim 49}$ (Ref. [21]) have also been reported in literature. Metastable cubic $Fe_{23}B_6$ and orthorhombic Fe_3B phases have also formed in a number of experiments [22–24].

We have undertaken a series of high-pressure experiments [25] aimed at the synthesis of the predicted boron-rich Fe-B phases (FeB_2 and FeB_4 [9]). Independent of pressure, a major component of the reacted mixture was stoichiometric FeB (Table S1, Ref. [25]). At low pressures (3 GPa and below) and temperatures of 1323 to 1973 K only known phases, orthorhombic FeB and rhombohedral $FeB_{\sim 49}$, were produced. Experiments at pressures of 8 to 18 GPa and temperatures of 1523 to 2023 K (Table S1 [25]) led to the synthesis of previously unidentified orthorhombic FeB_4, Fe_2B_7, and tetragonal $Fe_{1+x}B_{50}$ ($x \approx 0.04$) phases. The compounds crystallize from the melt and by optimizing the sample geometry, heating duration, and temperature gradients along the capsules it was possible to increase the amount of boron-rich Fe-B phases. However, as seen in Fig. 1(a), all the products of the high-pressure synthesis, and particularly FeB_4 and Fe_2B_7, are found in a tight mutual intergrowth, so that the procedure of phase separation is challenging.

We have manually selected small pieces of FeB_4 and carefully characterized them with x-ray diffraction, wavelength dispersive x-ray, and energy dispersive x-ray microprobe analysis (performed in SEM and TEM) [25] prior to further experiments. The largest pieces of phase-pure FeB_4 produced so far have dimensions on the order of $150 \times 150 \times 100$ μm^3. Maximal weight of phase-pure polycrystalline samples is of about 0.14 mg. We note, however, that standard characterization techniques are not sensitive enough to detect trace amounts of ferromagnetic impurities, such as metallic iron that is almost inevitably present in samples recovered after the high-pressure synthesis. These impurities are seen in magnetic susceptibility measurements (see [25]), but do not affect any of our conclusions regarding the superconductivity and superhardness of FeB_4.

The crystal structures of FeB_4, Fe_2B_7, and $Fe_{1+x}B_{50}$ have been solved from single crystal x-ray diffraction data (Table S2 [25]). A detailed description of Fe_2B_7 and $Fe_{1+x}B_{50}$ is out of the scope of the present Letter and will be published elsewhere.

According to the single crystal x-ray and electron diffraction [25], FeB_4 adopts an orthorhombic $Pnnm$ ($Z = 2$) crystal structure. The refined structure was confirmed by high-angle annular dark-field scanning transmission electron microscopy (HAADF-STEM) images along the [100], [010], and [001] directions [Fig. 1(b), Figs. S10, S11]. Additionally, planar defects confined to the (010) planes were occasionally observed in FeB_4. These defects are not abundant in the material, as indicated by the absence of any related diffuse intensity on the electron diffraction patterns (Fig. S9).

A polyhedral model of the FeB_4 structure is shown in Fig. 1(c) and Fig. S1 (Ref. [25]). The structure is remarkably close to that theoretically predicted [9] (Table S2 [25]), and found very recently also for CrB_4 [26,27].

Despite the very small size of the available phase-pure samples, we were able to confirm the prediction of superconductivity in FeB_4. While resistivity measurements are presently unfeasible, magnetic susceptibility data collected on polycrystalline samples indicate superconductivity in FeB_4. Magnetic susceptibility measurements under zero-field-cooling (ZFC) conditions reveal a strong diamagnetic response of FeB_4 samples below 3 K (Fig. 2). Above 3 K, FeB_4 is weakly paramagnetic with a nearly temperature independent susceptibility above 70 K. Additionally, our samples showed a weak ferromagnetic signal of unknown

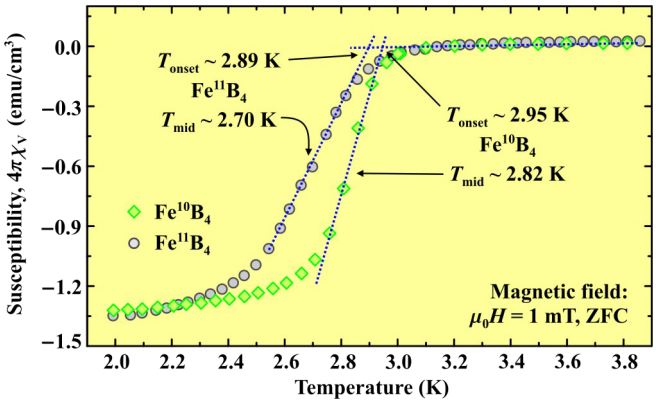

FIG. 2 (color online). Magnetic susceptibility of FeB_4 measured in an applied field of 1 mT ZFC. The susceptibility is normalized to the unit of volume (χ_V) and multiplied by 4π to facilitate the comparison with the expected value of $4\pi\chi_V = -1$ for the ideal superconductor with the demagnetization factor of $N = 0$. Two sets of data were collected on the samples enriched with ^{10}B and ^{11}B isotopes. Dashed lines denote the procedure for determining the onset temperature T_{onset} (see Ref. [25]). The midpoints of the susceptibility drop (T_{mid}) are shown as well.

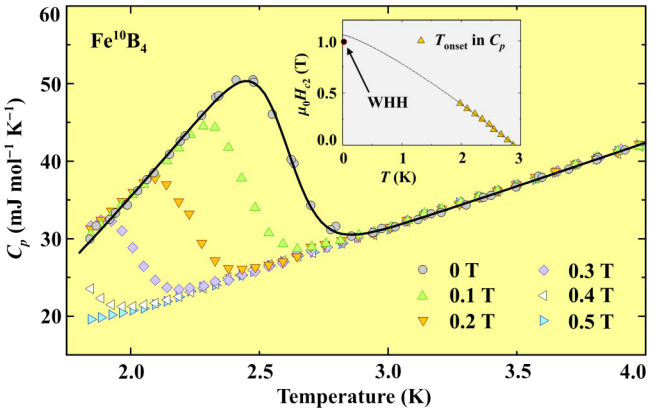

FIG. 3 (color online). Specific heat (C_p) of FeB_4 measured on the ^{10}B-enriched sample. The jump in C_p indicates the bulk superconductivity with $T_{onset} \sim 2.9$ K in zero field. External magnetic field shifts the transition to lower temperatures. The critical field H_{c2} estimated from T_{onset} in different fields is plotted as an inset and approximated by the empirical formula $H_{c2}(T) = H_{c2}(0)(1 - (T/T_c)^{\alpha})$ shown by the dashed line. The WHH estimate of $\mu_0 H_{c2}(0) = 1.0$ T is shown as well. In the main figure, the solid line is the BCS fit including a Gaussian broadening [30] (see text for details).

origin below 30 K. This signal is certainly extrinsic, because its magnitude varies from sample to sample (see [25]).

The strong diamagnetic response of FeB_4 is a clear footprint of superconductivity. The drop in the volume susceptibility (χ_V) is $4\pi(\Delta\chi_V) = -1.3$ that corresponds to the demagnetization factor of $N = 0.23$ according to $4\pi(\Delta\chi_V) = -1/(1 - N)$. This value of N is close to $N = 1/3$ expected for a spherical sample.

The bulk nature of superconductivity is confirmed by heat capacity measurements showing a jump at the superconducting transition around 3 K (Fig. 3). This jump is systematically shifted to lower temperatures in applied magnetic fields. Using the onset of superconductivity as a measure of T_c, we mapped the temperature dependence of the upper critical field H_{c2}. It increases upon cooling, with an initial slope of $\mu_0 dH_{c2}/dT = -0.5$ T/K at $T_c(0) \sim 2.9$ K. At lower temperatures, $H_{c2}(T)$ bends downwards. The critical field at zero temperature is extrapolated as $\mu_0 H_{c2}(0) = -0.693 T_c \mu_0 (dH_{c2}/dT) \sim 1.0$ T according to the Werthamer-Helfand-Hohenberg formula [28]. Alternatively, $H_{c2}(0)$ can be determined from a fit with the empirical formula $H_{c2}(T) = H_{c2}(0) \times (1 - (T/T_c)^{\alpha})$ yielding $\mu_0 H_{c2}(0) = 1.05$ T and $\alpha = 1.25$. Both estimates of $H_{c2}(0)$ are far below the Pauli-paramagnetic limit for weak electron-phonon coupling $\mu_0 H_{c2}[\text{Tesla}] = 1.86 T_c[\text{Kelvin}] \sim 5.4$ T [29] and corroborate phonon-mediated superconductivity in FeB_4. In contrast, unconventional superconductors may have critical fields above the Pauli-paramagnetic limit.

To elucidate the nature of the observed superconducting transition, we compared the transition temperatures in the samples containing different boron isotopes (Fig. 2). The sample enriched with the heavier B isotope shows a lower T_c (2.95 and 2.89 K for T_{onset} or 2.82 and 2.70 K for T_{mid} in the ^{10}B and ^{11}B samples, respectively), as expected for a phonon-mediated superconductor. Indeed, our tentative estimate of the isotope effect [25] yields $\Delta T_c \sim 0.05$ K in good agreement with $\Delta T_c \sim 0.06$–0.12 K, as found experimentally. Specific heat data provide further evidence for phonon-mediated superconductivity. The specific heat of the normal state, as measured in the applied field of 1 T, follows $C_p = \gamma_n T + \beta T^3$ with $\gamma_n = 10.2(2)$ mJ mol^{-1} K^{-2} and $\beta = 0.025(1)$ mJ mol^{-1} K^{-4} determined from the fit of C_p/T vs T^2 up to $T = 12$ K (see [25], Fig. S8). This β value yields the quite high Debye temperature $\theta_D \sim 730$ K indicating predominantly hard phonons, which are indeed expected for superhard FeB_4 (see below). The value of γ_n corresponds to $N(E_F) = 4.3$ states eV^{-1} (f.u.)$^{-1}$ at the Fermi level and suggests a strong renormalization of the electronic DOS compared to the LDA result of $N(E_F) \sim 1$ state eV^{-1} (f.u.)$^{-1}$ [9]. At zero field, the jump in C_p at the superconducting transition is $\Delta C_p \sim 35$ mJ/mol K yielding $\Delta C_p/\gamma_n T_c \sim 1.18$ in reasonable agreement with 1.43 expected for the BCS limit with weak electron-phonon coupling. The proximity of ΔC_p to the BCS value is indicative of the conventional, phonon-mediated superconductivity in FeB_4. This finding is further corroborated by a fit of the zero-field $C_p(T)$ with the BCS expression by Mühlschlegel [30] yielding $\gamma_n = 8.8(1)$ mJ mol^{-1} K^{-2} in reasonable agreement with γ_n derived from the 1 T data.

Metal borides are known for their high hardness [31], so that characterization of the elastic behavior of the newly synthesized boride and its stability under pressure is an

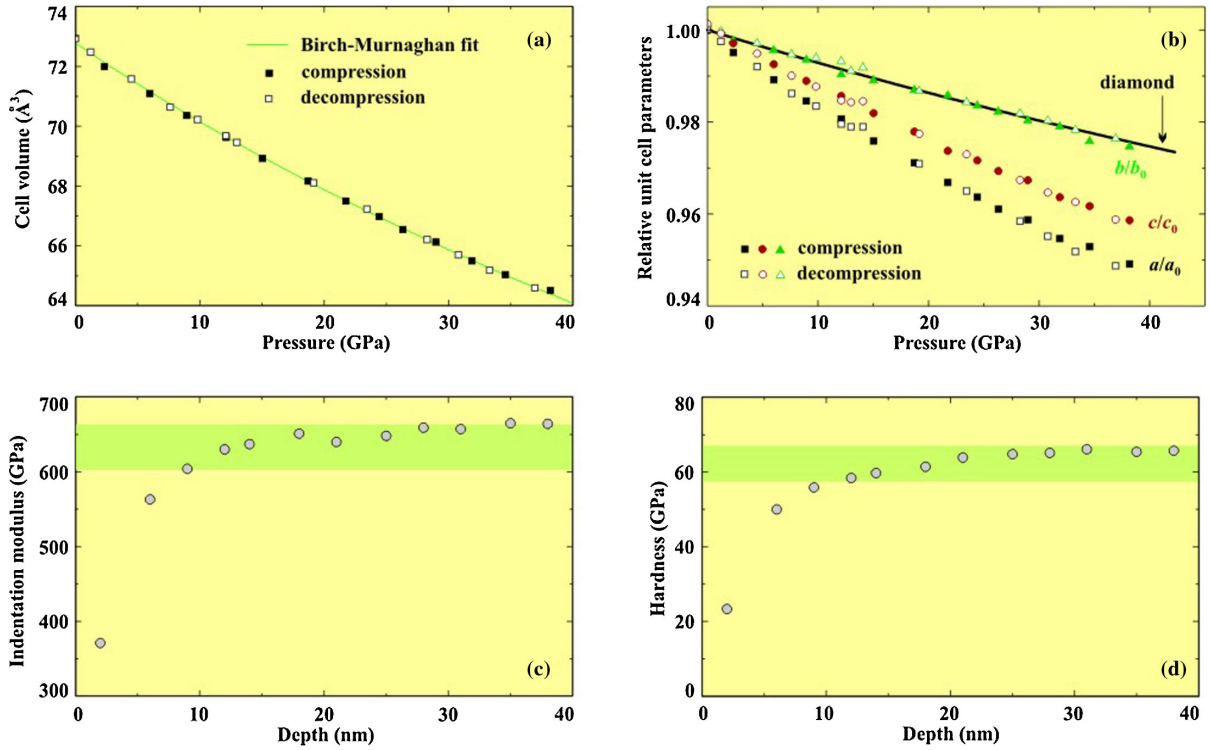

FIG. 4 (color online). Compressibility of FeB_4 and the results of nanoindentation measurements. (a) The pressure dependence of the unit cell volume based on single crystal x-ray diffraction data. The fit of the pressure-volume data with the third-order Birch-Murnaghan equation of state (solid line) gave the bulk modulus $K = 252(5)$ GPa, $K' = 3.5(3)$, and $V_0 = 72.79(4)$ Å^3/unit cell. (b) The relative changes of the unit cell parameters as a function of pressure. The stiffness of the FeB_4 structure along the b direction is the same as that of diamond (continuous line according to Ref. [32]). Closed symbols represent the data points obtained on compression, and open ones—on decompression. The uncertainties are not shown since they are smaller than the size of symbols. (c) Depth dependent average values of indentation modulus. (d) Hardness of FeB_4. Load-displacement curves without pop-ins have been used for evaluation with tip compression correction.

important issue. No phase transitions were observed under compression of FeB_4 at ambient temperature in a diamond anvil cell up to about 40 GPa [25]. Compressibility measurements on both compression and decompression revealed the remarkably high bulk modulus, $K = 252(5)$ GPa [$K' = 3.5(3)$, $V_0 = 72.79(4)$ Å] [Fig. 4(a)], and a significant degree of anisotropy in the elastic behavior of FeB_4. The structure of FeB_4 is most compressible along the a direction, while stiffest along the b axis [Fig. 4(b)]. It may be related to the fact that the shortest (and thus least compressible) B-B contact [1.714(6) Å at ambient conditions] in this structure is almost parallel to the b axis. The stiffness of the FeB_4 structure along the b direction is the same as that of diamond [32] [Fig. 4(b)] suggesting that the iron tetraboride may have remarkably advanced mechanical properties. Figures 4(c) and 4(d) present the results, which are obtained by an average over several nanoindentation load-displacement charts on FeB_4 without the feature of a pop-in [25]. The depth dependent indentation or reduced modulus E_r shows a clear plateau with $E_r = 633 \pm 30$ GPa [Fig. 4(c)] that is far ahead compared to common ceramic materials like alumina [33] (~350 GPa) at room temperature. However, Young's moduli of diamond [34] (~1000 GPa) and cubic boron nitride [35] (~900 GPa) are still considerably larger. Nevertheless the nanoindentation hardness approaches an average value of 62 ± 5 GPa [Fig. 4(d)]. Microhardness measurements were difficult to conduct because of the small size of the phase-pure samples of FeB_4. However, several successful tests (Fig. S2) with a load of 20 N gave values of the Vickers hardness ranging from 43 to 70 GPa, thus confirming that FeB_4 belongs to the group of superhard materials [36].

In summary, we have prepared and characterized the novel superhard superconductor FeB_4. Our data not only support the predicted orthorhombic crystal structure [9], but also confirm the superconductivity of FeB_4 that was likewise predicted theoretically. We argue that the superconductivity of FeB_4 is mediated by phonons, which is highly unusual for Fe-based materials [2,4]. In addition, the FeB_4 compound was found to be superhard, well exceeding the expectations about its potential mechanical properties [26]. This finding, bridging the gap between the superhardness and superconductivity community, may lead, for example, to a possibility for designing new superconducting nanoelectromechanical systems and/or observation of new fundamental effects.

The work was supported by the German Research Foundation (DFG). N. D. thanks DFG for financial support through the Heisenberg Program and the DFG Project DU 954-8/1. H. G. gratefully acknowledges financial support of the Alexander von Humboldt Foundation. A. M. A., D. B., and G. V. T. acknowledge support from the ERC Grant No. 246791 "COUNTATOMS". A. A. T. was partly supported by the MTT77 Mobilitas Grant of the ESF.

L. D., N. D., and A. N. K. conceptualized the work. L. D. and N. D. planned and coordinated the study. H. G. conducted all synthesis experiments and analyzed all samples; E. B. analyzed all single crystal x-ray diffraction data; A. A. T., D. K., and W. S. performed magnetic susceptibility and heat-capacity measurements and analyzed the data; experiments in DAC were carried out by E. B., M. M., M. H., L. D., and N. D.; A. M. A., D. B., and G. V. T. performed the TEM analysis; A. R. conducted nanoindentation measurements. Y. N. performed the microprobe analysis. The paper was prepared by N. D. with contributions of all authors.

*natalia.dubrovinskaia@uni-bayreuth.de

[1] S. W. Woodley and R. Catlow, Nat. Mater. **7**, 937 (2008).
[2] I. I. Mazin, Nature (London) **464**, 183 (2010).
[3] G. Hautier, A. Jain, and S. P. Ong, J. Mater. Sci. **47**, 7317 (2012).
[4] M. L. Cohen, J. Mater. Res. **26**, 2815 (2011).
[5] M. Lüders, M. A. L. Marques, N. N. Lathiotakis, A. Floris, G. Profeta, L. Fast, A. Continenza, S. Massidda, and E. K. U. Gross, Phys. Rev. B **72**, 024545 (2005).
[6] A. N. Kolmogorov, M. Calandra, and S. Curtarolo, Phys. Rev. B **78**, 094520 (2008).
[7] K. J. Chang and M. L. Cohen, Phys. Rev. B **30**, 5376 (1984).
[8] J. B. Neaton and N. W. Ashcroft, Nature (London) **400**, 141 (1999).
[9] A. N. Kolmogorov, S. Shah, E. R. Margine, A. F. Bialon, T. Hammerschmidt, and R. Drautz, Phys. Rev. Lett. **105**, 217003 (2010).
[10] K. Burke, J. Chem. Phys. **136**, 150901 (2012).
[11] P. B. Allen and B. Mitrovic, Solid State Phys. **37**, 1 (1983).
[12] J. Nagamatsu, N. Nakagawa, T. Muranaka, Y. Zenitani, and J. Akimitsu, Nature (London) **410**, 63 (2001).
[13] I. I. Mazin, D. A. Papaconstantopoulos, and M. J. Mehl, Phys. Rev. B **65**, 100511 (2002).
[14] G. K. Shenoy, D. R. Noakes, and G. P. Meisner, J. Appl. Phys. **53**, 2628 (1982).
[15] Y. Nakai, K. Ishida, D. Kikuchi, H. Sugawara, and H. Sato, J. Phys. Soc. Jpn. **74**, 3370 (2005).
[16] J. L. Smith, J. C. Lashley, H. M. Volz, R. A. Fisher, and P. S. Riseborough, Philos. Mag. **88**, 2847 (2008).
[17] A. F. Bialon, T. Hammerschmidt, R. Drautz, S. Shah, E. R. Margine, and A. N. Kolmogorov, Appl. Phys. Lett. **98**, 081901 (2011).
[18] H. Okamoto, J. Phase Equilib. Diffus. **25**, 297 (2004).
[19] C. Kapfenberger, B. Albert, R. Pöttgen, and H. Huppertz, Z. Kristallogr. **221**, 477 (2006).
[20] L. G. Voroshnin, L. S. Lyakhovich, G. G. Panich, and G. F. Protasevich, Metal Sci. Heat Treat. **12**, 732 (1970).
[21] B. Callmer and T. Lundstroem, J. Solid State Chem. **17**, 165 (1976).
[22] Y. Khan, E. Kneller, and M. Sostarich, Z. Metallkd. **73**, 624 (1982).
[23] B. Yao, W. H. Su, F. S. Li, B. Z. Ding, and Z. Q. Hu, J. Mater. Sci. Lett. **16**, 1991 (1997).
[24] V. A. Barinov, V. I. Voronin, V. T. Surikov, V. A. Kazantsev, V. A. Tsurin, V. V. Fedorenko, and S. I. Novikov, Phys. Metals Metallography **100**, 456 (2005).
[25] See the Supplemental Material at http://link.aps.org/supplemental/10.1103/PhysRevLett.111.157002 for experimental details and technical procedures.
[26] H. Niu, J. Wang, X. Q. Chen, D. Li, Y. Li, P. Lazar, R. Podloucky, and A. N. Kolmogorov, Phys. Rev. B **85**, 144116 (2012).
[27] A. Knappschneider *et al.*, Inorg. Chem. **52**, 540 (2013).
[28] N. R. Werthamer, E. Helfand, and P. C. Hohenberg, Phys. Rev. B **147**, 295 (1966).
[29] B. S. Chandrasekhar, Appl. Phys. Lett. **1**, 7 (1962).
[30] B. Mühlschlegel, Z. Phys. **155**, 313 (1959).
[31] B. Albert and H. Hillebrecht, Angew. Chem., Int. Ed. Engl. **48**, 8640 (2009).
[32] F. Occelli, P. Loubeyre, and R. Letoullec, Nat. Mater. **2**, 151 (2003).
[33] *Materials Science and Engineering Handbook*, edited by W. Alexander and J. F. Shackelford (CRC Press, Boca Raton, 2000), 3rd ed.
[34] N. Dubrovinskaia, S. Dub, and L. S. Dubrovinsky, Nano Lett. **6**, 824 (2006).
[35] R. Haubner, M. Wilhelm, R. Weissenbacher, and B. Lux, High Performance Non-Oxide Ceramics II, Structure and Bonding **102**, 1 (2002).
[36] V. Brazhkin, N. Dubrovinskaia, M. Nicol, N. Novikov, R. Riedel, V. Solozhenko, and Y. Zhao, Nat. Mater. **3**, 576 (2004).